IFIC/15-80

QCD running in neutrinoless double beta decay: Short-range mechanisms

M. González* and S.G. Kovalenko†
Universidad Técnica Federico Santa María, Centro-Científico-Tecnológico de Valparaíso, Casilla 110-V, Valparaíso, Chile

M. Hirsch‡
AHEP Group, Instituto de Física Corpuscular – C.S.I.C./Universitat de València Edificio de Institutos de Paterna, Apartado 22085, E–46071 València, Spain

Abstract

The decay rate of neutrinoless double beta ($0\nu\beta\beta$) decay contains terms from heavy particle exchange, which lead to dimension-9 ($d = 9$) six fermion operators at low energies. Limits on the coefficients of these operators have been derived previously neglecting the running of the operators between the high-scale, where they are generated, and the energy scale of double beta decay, where they are measured. Here we calculate the leading order QCD corrections to all possible d=9 operators contributing to the $0\nu\beta\beta$ amplitude and use RGE running to calculate 1-loop improved limits. Numerically, QCD running changes limits by factors of the order of or larger than typical uncertainties in nuclear matrix element calculations. For some specific cases, operator mixing in the running changes limits even by up to two orders of magnitude. Our results can be straightforwardly combined with new experimental limits or improved nuclear matrix element calculations to re-derive updated limits on all short-range contributions to $0\nu\beta\beta$ decay.

Keywords: double beta decay, physics beyond the standard model, neutrinos

*Electronic address: marcela.gonzalez@postgrado.usm.cl
†Electronic address: Sergey.Kovalenko@usm.cl
‡Electronic address: mahirsch@ific.uv.es

I. INTRODUCTION

Absence of neutrinoless double beta ($0\nu\beta\beta$) decay constrains lepton number violating extensions of the Standard Model (SM). Usually lower limits on $0\nu\beta\beta$ decay half-lives are interpreted as upper limits on the effective Majorana neutrino mass, $\langle m_\nu \rangle = \sum_j m_j U_{ej}^2$, but many models generating a non-zero $0\nu\beta\beta$ decay amplitude not directly proportional to $\langle m_\nu \rangle$ have been discussed in the literature, for recent reviews on $0\nu\beta\beta$ decay see for example [1, 2].

One can classify the different contributions to the general $0\nu\beta\beta$ decay rate either as long-range [3] or as short-range [4] contributions. The long-range part of the amplitude describes the exchange of a light neutrino between two point-like vertices. If both vertices are the SM charged current vertices, the resulting diagram corresponds to the well-known mass mechanism, but other long range contributions, not directly proportional to $\langle m_\nu \rangle$, do exist in many models, like for example R-parity violating SUSY [5–7] or leptoquark models [8].

The short-range part of the $0\nu\beta\beta$ amplitude is due to "heavy" particle exchange. [1] After integrating them out the amplitude can be represented as (the nuclear matrix element of) a true dimension-9 ($d = 9$) quark-level effective operator, which can be schematically written as:

$$\mathcal{O}_{d=9} \propto \frac{1}{\Lambda_{\rm LNV}^5} \bar{u}\bar{u}\, dd\, \bar{e}\bar{e} \ . \tag{1}$$

The general $SU(3)_c \times SU(2)_L \times U(1)_Y$ invariant decomposition of this $d = 9$ operator has been discussed in [9]. The tables given in [9] can be understood as a summary of all (proto-) models which contribute to $0\nu\beta\beta$ decay at tree-level based on scalar exchange. Once all possible UV-completions of eq.(1) have been specified, one can then use the results of [4] to derive general limits on all possible models contributing to $0\nu\beta\beta$ decay.

Given current experimental lower limits on half-lives of $0\nu\beta\beta$ decay, of the order of (few) 10^{25} ys for ^{76}Ge [10] and ^{136}Xe [11–13], the energy scale, $\Lambda_{\rm LNV}$, at which eq.(1) is generated is expected to be of the order of roughly $\mathcal{O}$(TeV). On the other hand, $0\nu\beta\beta$ decay is a low-energy process with the typical momentum scale given by the Fermi momentum of nucleons, p_F. This rather large mismatch in scales implies that the running of the operators may be quite important numerically. This observation forms the basic motivation for the current paper.

Calculations of RGE ("renormalization group equation") improved Wilson coefficients for weak decay operators have become standard tools [14, 15] in electro-weak precision physics. Here, we calculate the leading order QCD diagrams, correcting eq.(1), and use RGE running for all possible $d = 9$ operators contributing to $0\nu\beta\beta$ decay. Colour mismatched operators, which appear in this calculation, lead to operator mixing. Since different operators in $0\nu\beta\beta$ decay can have vastly different nuclear matrix elements, this effect in some case leads to

[1] Any particle with mass larger than the typical Fermi momentum of the nucleons, i.e. $\mathcal{O}(0.1)$ GeV, can be considered "heavy" in $0\nu\beta\beta$ decay. All exotic fermions contributing to the short-range amplitude, except possibly sterile neutrinos, are expected to have masses larger than $\mathcal{O}$(100 GeV).

a rather drastic change in the derived limits. It is therefore important to take these QCD corrections into account in the calculation of limits on short-range operators.

We note, that our paper is not the first to consider QCD corrections. In [16] the author calculated Wilson coefficients for currents of the form $V+A$ and $V-A$ and mentions that colour mismatch is expected to be important for $S \pm P$. Reference [17] consider a particular scalar model for $0\nu\beta\beta$ decay and calculates QCD corrections for $S \pm P$ for the pion exchange mechanism. Our current paper, however, is the first one to give the complete set of QCD corrections to all short-range operators.

The rest of this paper will be organized as follows. In the next section we will first repeat the most important definitions for operators, currents and the $0\nu\beta\beta$ decay half-life given in [4], before summarizing in section III briefly how to connect low-energy $0\nu\beta\beta$ decay with the possible ultra-violet completions ("models") of the $d = 9$ operator [9]. Section IV gives a description of our calculational procedure, defining the Wilson coefficients and basic formulas for the RGE running. Section V then discussed our numerical results, before we close with a short summary in section VI.

II. LOW-ENERGY EFFECTIVE LAGRANGIAN AND $0\nu\beta\beta$-DECAY HALF-LIFE

From the low-energy point of view, adequate for the energy scale $\mu_{\beta\beta}$ of $0\nu\beta\beta$ decay, the short range (SR) part of the decay amplitude can be derived from the generic effective Lagrangian [4] [2]

$$\mathcal{L}_{\rm eff}^{0\nu\beta\beta} = \frac{G_F^2}{2m_p} \sum_{i,XY} C_i^{XY}(\mu) \cdot \mathcal{O}_i^{XY}(\mu), \tag{2}$$

with the operator basis containing the following operators, classified by their Lorentz structure:

$$\begin{aligned}
\mathcal{O}_1^{XY} &= 4(\bar{u}P_X d)(\bar{u}P_Y d)\ j, && (3)\\
\mathcal{O}_2^{XX} &= 4(\bar{u}\sigma^{\mu\nu}P_X d)(\bar{u}\sigma_{\mu\nu}P_X d)\ j, && (4)\\
\mathcal{O}_3^{XY} &= 4(\bar{u}\gamma^{\mu}P_X d)(\bar{u}\gamma_{\mu}P_Y d)\ j, && (5)\\
\mathcal{O}_4^{XY} &= 4(\bar{u}\gamma^{\mu}P_X d)(\bar{u}\sigma_{\mu\nu}P_Y d)\ j^{\nu}, && (6)\\
\mathcal{O}_5^{XY} &= 4(\bar{u}\gamma^{\mu}P_X d)(\bar{u}P_Y d)\ j_{\mu} && (7)
\end{aligned}$$

with $X, Y = L, R$ and the leptonic currents are

$$j = \bar{e}(1 \pm \gamma_5)e^c\,, \quad j_\mu = \bar{e}\gamma_\mu\gamma_5 e^c. \tag{8}$$

Note that, leptonic currents $\bar{e}\gamma^\mu e^c$, $\bar{e}\sigma^{\mu\nu}e^c$ and $\bar{e}\sigma^{\mu\nu}\gamma_5 e^c$ vanish identically. Note further that the factor $\frac{G_F^2}{2m_p}$ in Eq. (2) has been chosen to make the coefficients C_i dimensionless quantities

[2] In [4] the coefficients in Eq. (2) where denoted as ϵ_i^{XY}.

and we have introduced a factor of 4 in Eqs. (3)-(7), such that the numerical values of C_i can be directly compared with the numbers given in the original paper [4]. Finally, all hadronic operators can have superscripts LL, LR or RR, with the exception of $\mathcal{O}_2^{XX}$, for which $\mathcal{O}_2^{LR} = \mathcal{O}_2^{RL} \equiv 0$.

Eq. (2) is nothing but the most general parametrization of the effective Lagrangian in terms of the quark-lepton operators, which can contribute to the $0\nu\beta\beta$ decay amplitude at tree level. No particular physics underlying the Lagrangian (2) is implied at this stage. Note that the Lagrangian (2) is tied to the typical energy scale $\mu \sim p_F$ of $0\nu\beta\beta$ decay, which is of the order of the Fermi momentum of nucleons and quarks in $0\nu\beta\beta$ decaying nucleus, $p_F \sim 100$ MeV. The Lagrangian (2) can be applied to processes with any hadronic states: quarks, mesons, nucleons, other baryons and nuclei. The corresponding amplitude is determined by the matrix elements of the hadronic part $\mathcal{O}_i^{\rm h}$ of the operators in Eqs. (3)-(7) and coefficients C_i independent of the low-energy scale non-perturbative hadronic dynamics. This is the well-recognizable feature of the Operator Product Expansion (OPE), representing interactions of some high-scale renormalizable model in the form of Eq. (2) below a certain scale μ. The coefficients C_i are known as Wilson coefficients, depending on the parameters of a high-scale model.

Applying standard nuclear theory methods, one finds for the half-life:

$$\left[T_{1/2}^{0\nu\beta\beta}\right]^{-1} = G_1 \left|\sum_{i=1}^{3} C_i(\mu_0)\mathcal{M}_i\right|^2 + G_2 \left|\sum_{i=4}^{5} C_i(\mu_0)\mathcal{M}_i\right|^2 \tag{9}$$

Here, $G_1 = G_{01}$ and $G_2 = (m_e R)^2 G_{09}/8$ are phase space factors in the convention of [18], and $\mathcal{M}_i = \langle A_f|\mathcal{O}_i^{\rm h}|A_i\rangle$ are the nuclear matrix elements defined in Ref. [4]. In the above equation the summation over the coefficients corresponding to the operators $\mathcal{O}_i^{XY}$ with different chiralities $X, Y = L, R$ is implied. The Wilson coefficients $C_i(\mu_0)$ should be taken close to the typical $0\nu\beta\beta$-energy scale. In our analysis we choose $\mu_0 = 1$GeV. In Eq. (9) we have not included interference terms, given in Eq.(3) of Ref. [4], since none of the high-scale models listed in [9] mixes the coefficients $C_{1,2,3}$ with $C_{4,5}$.

Numerical values for the nuclear matrix elements $\mathcal{M}_i$, based on the pn-QRPA approach of [19], can be found for ^{76}Ge in [4], for other isotopes of interest see [2]. It is, however, well-known that nuclear matrix elements for $0\nu\beta\beta$ decay have quite large numerical uncertainties. Recent publications calculating matrix elements for heavy neutrino exchange, i.e. matrix elements for the short-range part of the amplitude corresponding in our notation to the term C_3^{LL}, give numerical values which are larger than those of [2] by typically 50 % (40 %) in the QRPA calculation by the Tübingen group [20] (Jyväskylä group [21]). Shell model calculations for light neutrino exchange, on the other hand, seem to give matrix elements which are up to a factor of two smaller than those of QRPA [22]. Similar factors are found for heavy neutrino exchange in the shell model calculation of [23]. However, a recent shell model calculation for ^{76}Ge gives matrix elements for light neutrino exchange [24] only 15-40 % smaller than than those of [19]. While these variations in numerical results do probably not cover the error bar in the calculation of nuclear matrix elements completely, from these

numbers one may estimate that currently matrix elements for the short-range part have uncertainties of roughly a factor of 2 or so.

We note, however, that while we do use the numerical values of [2] for the derivation of new limits, all our calculations are presented in such a way that the running of the operators is separated completely from the nuclear structure part of the calculation. Thus, our coefficients can be combined with any new nuclear matrix element calculations, should they become available, to extract updated limits.

III. LINK TO HIGH-SCALE MODELS

As already mentioned above, Eq. (2) is a general parametrization of all the possible contact interactions contributing to $0\nu\beta\beta$ decay amplitude at tree level, without referring to any underlying physics. The latter is typically thought to be represented by renormalizable models with heavy degrees of freedom which decouple from the light sector at certain energy scale (much) larger than the characteristic scale of $0\nu\beta\beta$ decay. In the literature one can find two approaches connecting the effective Lagrangian (2) to such high-energy models. We will discuss them briefly.

Historically, the first approach was the top-down approach: Starting from a concrete high-scale model and integrating out heavy degrees of freedom of a mass M_h at energy-scales $\mu < M_h$. Then, there appear effective non-renormalizable interactions of the light fields in the form of an expansion in the inverse powers of M_h, which is the operator product expansion. The interactions (2) are then the leading d=9 terms of this expansion. The well-known and simplest example of such a model is the SM, extended by a heavy Majorana neutrino N with the mass $M_N \gg \mu_{\beta\beta} \sim p_F \sim 100$ MeV. The relevant Lagrangian term is

$$\mathcal{L}_{\rm SMN} = \frac{g_2}{\sqrt{2}}\,\overline{e_L}\,\gamma^\mu U_{eN} N \cdot W^-_\mu \tag{10}$$

where g_2 is the $SU(2)_L$ gauge coupling constant and U_{eN} describes the mixing of this heavy state with the ordinary electron neutrino. The tree-level diagram contributing to the $0\nu\beta\beta$ amplitude is shown in Fig. (1) on the left with $W^\pm$ denoted by dashed lines. At momenta p of the external legs below both M_W and M_N one can expand the corresponding propagators in p^2/M_i^2 with $i = W, N$. The leading term is

$$\mathcal{L}^{\rm eff}_{SMN} = -8\frac{G_F}{\sqrt{2}}\frac{U_{eN}}{M_N}\,\overline{u_L}\,\gamma_\mu d_L \cdot \overline{u_L}\,\gamma_\mu d_L \cdot \bar{e} P_R e^c. \tag{11}$$

In the path integral approach the described procedure is equivalent to integrating out the W and N fields, which consists of neglecting their kinetic terms, justified at energies below their masses, and the subsequent Gaussian integration over W and N variables. (For a pedagogical review see Refs. [14, 15]). In the literature a great host of high-scale models have been linked to the form of the Lagrangian (2) in this way. The key point here is that there are at least two orders of magnitude of hierarchy between the scale where the new degrees of freedom are integrated out and the scale of $0\nu\beta\beta$ decay, which the parameterization of Eq. (2) is

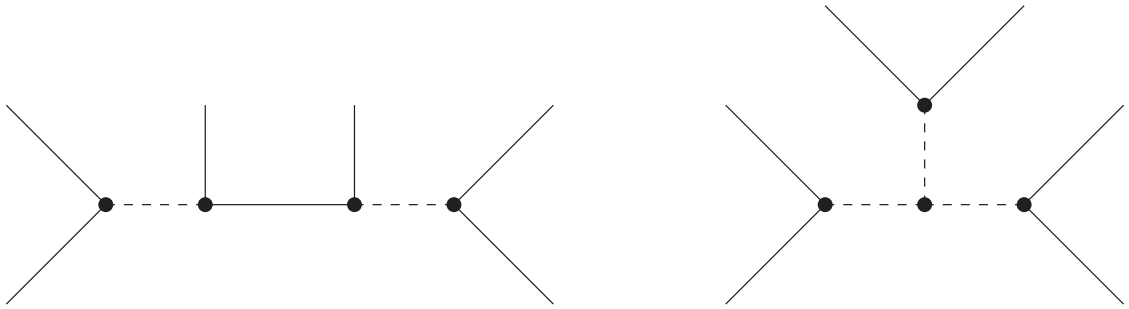

FIG. 1: Tree-level topologies contributing to the $0\nu\beta\beta$ decay rate. To the left T-I, scalar-fermion-scalar exchange; to the right T-II, scalar-scalar-scalar diagrams. Scalars could also be replaced by vectors.

tied to. As has been pointed out for the first time in ref. [16] in the presence of QCD loop corrections such a scale hierarchy has a significant impact on the relation of the parameters of high-scale models and the parameters C_i extracted from the measurements of $0\nu\beta\beta$ decay half-life on the basis of Eq. (9).

Recently, a bottom-up approach to "deconstructing" $0\nu\beta\beta$ decay has been proposed in Ref. [9]. This "decomposition" approach to Eq. (1) surveys in a generic way all possible renormalizable $SU(3)_c \times SU(2)_L \times U(1)_Y$ invariant interactions leading in the low energy limit to the effective operators in Eq. (2). As shown in [9], there are only two tree-level topologies for the decomposition of the operator in Eq. (2). These are shown in Fig. (1) and denoted T-I and T-II. The six outside lines stand for any of $\bar{u}$, d or $\bar{e}$. Dashed lines are for bosons (either scalars or vectors), the full (inner) line in T-I is for some exotic (i.e. non-standard model) fermion.

The task of defining all possible ultra-violet completions ("models") contributing to the $0\nu\beta\beta$ decay rate (at tree-level), then reduces the problem to finding all SM-invariant fermion bilinears involving the quarks and leptons (plus all bilinears involving one SM fermion and one exotic fermion in case of T-I) of Eq. (1) and, after integrating out all heavy (ie. beyond SM) particles, rewrite the resulting expressions into the basis operators of Eq. (2). We will discuss one simple example here, all other possible decompositions can be found analogously. Concentrating on only the scalar case and taking into account all possible variations there is a total of 135 (T-I) plus 27 (T-II) possible assignments, complete lists are given in the Tables of [9].

To make contact with [9], we will discuss here a simple example based on the decomposition T-I-1-i. This corresponds to the fermions in Fig. (1) left assigned as $(\bar{u}_L d_R)(\bar{e}_L)(\bar{e}_L)(\bar{u}_L d_R)$. With this choice, the two scalars are $S_1 = S_2$ and are fixed to be either $S_{1,2,1/2}$ or $S_{8,2,1/2}$. For the former the intermediate fermion is either $\psi_{1,1,0}$ or $\psi_{1,3,0}$, while for the latter it is fixed to $\psi_{8,1,0}$ or $\psi_{8,3,0}$. Interactions appearing in the diagram are

then given by:

$$\begin{aligned}\mathcal{L}_Y &= Y_{Qd(1)}(\bar{Q}d_R)S_{1,2,1/2} + Y_{Qd(8)}(\bar{Q}d_R)(\lambda^A/2)S_{8,2,1/2} \\ &+ Y_{e\psi(1)}(\bar{e}_L\psi_{1,X,0})S^\dagger_{1,2,1/2} + Y_{e^c\psi(1)}(\bar{e}^c_L\psi_{1,X,0})S_{1,2,1/2} \\ &+ Y_{e\psi(8)}(\bar{e}_L\psi_{8,X,0})(\lambda^A/2)S^\dagger_{8,2,1/2} + Y_{e^c\psi(8)}(\bar{e}^c_L\psi_{8,X,0})(\lambda^A/2)S_{8,2,1/2}\end{aligned} \tag{12}$$

Here, (λ^A) are the Gell-Mann matrices, and $Y_{ab(C)}$ some unknown Yukawa couplings. Eq. (12), together with the Majorana propagator for $\psi_{C,X,0}$ and after integrating out heavy particles, gives an effective Lagrangian, which for the colour octet case reads

$$\mathcal{L}_{eff} = \frac{Y^2_{Qd(8)}Y_{e\psi(8)}Y_{e^c\psi(8)}}{m^4_{S_{8,2,1/2}}m_{\psi_{8,X,0}}}(\lambda^A/2)^b_a(\lambda^A/2)^d_c(\bar{Q}^a d_{R,b})(\bar{Q}^c d_{R,d})(\bar{e}P_R e^c). \tag{13}$$

The Lagrangian for the color singlet case is identical to Eq. (13) after some obvious replacements, i.e. $(\lambda^A/2)^i_j \to 1$ etc. It is also already in the basis defined in Eq. (2), so for the colour-singlet case only

$$C_1^{RR} = \left(\frac{2m_p}{G_F^2}\right)\frac{Y^2_{Qd(1)}Y_{e\psi(1)}Y_{e^c\psi(1)}}{m^4_{S_{1,2,1/2}}m_{\psi_{1,X,0}}}$$

is non-zero. For the colour octet, however, before applying the standard non-relativistic impulse approximation to convert quark to nucleon currents, first the color singlet has to be extracted. Using

$$(\lambda^A)^a_b(\lambda^A)^c_d = -\frac{2}{3}\delta^a_b\delta^c_d + 2\delta^a_d\delta^c_b,$$

this leads to an operator, which contains the original operator plus a color mismatched piece:

$$-\frac{2}{3}(\bar{Q}^a d_{R,a})(\bar{Q}^a d_{R,a}) + 2(\bar{Q}^a d_{R,b})(\bar{Q}^b d_{R,a}). \tag{14}$$

This can be brought to canonical form using Fierz rearrangement, resulting in:

$$\mathcal{L}_{eff} \propto C_1^{RR}\Big(-\frac{5}{3}\mathcal{O}_1^{RR} - \frac{1}{4}\mathcal{O}_2^{RR}\Big). \tag{15}$$

Thus, C_1^{RR} in this case is determined by a sum of two of the basic operators. We will discuss how to take into account the appearance of two operators in section (V), where our numerical results are presented. Note that in the list of [9] all high scale model lead to at most two different operator in the low-energy decay rate.

IV. OPE AND QCD EFFECTS

In this section we develop the formalism for taking into account the Leading Order (LO) QCD corrections to the operator product expansion given in Eq. (2). We follow essentially the methods described in the reviews [14, 15] for semi-leptonic and hadronic decays of mesons. An important feature of the representation of the effective Lagrangian, see Eq. (2), is that it involves the complete set of d=9 operators (3)-(7) contributing to $0\nu\beta\beta$ decay. Therefore, no new operators are generated under renormalization.

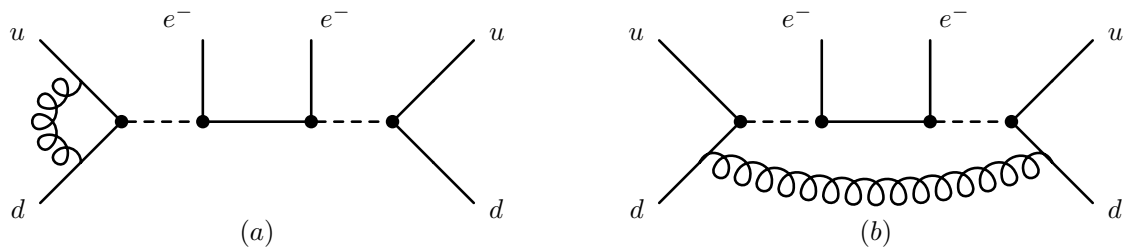

FIG. 2: $0\nu\beta\beta$ decay example diagrams of one-loop QCD corrections to the "full theory"

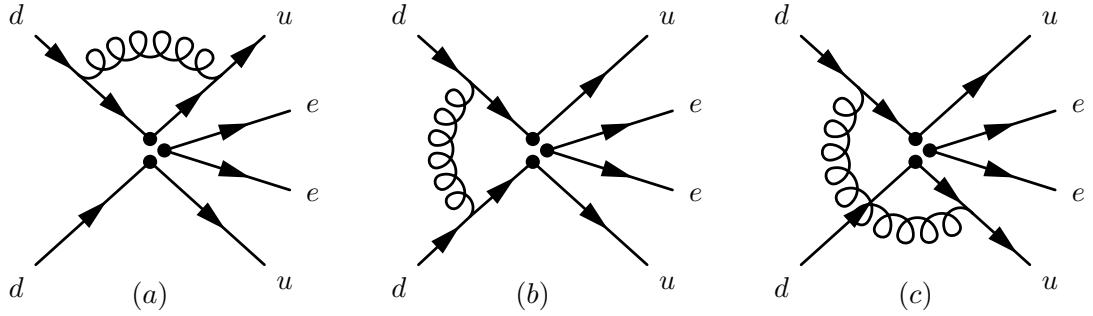

FIG. 3: One-loop QCD corrections to the short range mechanisms of $0\nu\beta\beta$ decay in the effective theory.

A. Matching of Full Theory onto Effective

We start with the discussion of the procedure relating the high-scale renormalizable model, typically dubbed in the present context as a "full theory", to an effective theory with the Lagrangian Eq. (2) treated as the low-energy limit of the full theory. This matching procedure allows one to derive the coefficients C_i in terms of the parameters of the high-scale model and take into account the corresponding perturbative QCD effects. The matching is settled at the level of amplitudes of the full theory $\mathcal{A}_{full}$ and of the effective one $\mathcal{A}_{eff} \sim \langle \mathcal{L}_{\rm eff}^{0\nu\beta\beta} \rangle$ requiring they coincide

$$\mathcal{A}_{full} = \frac{G_F^2}{2m_p} \sum_i C_i(\mu) \cdot \langle \mathcal{O}_i(\mu) \rangle \tag{16}$$

at an energy scale $\mu \leq \Lambda$ below the heavy particle masses of the full theory. This is the so-called matching condition. In the left-hand side of this equation only the leading term $\sim (1/\Lambda)^5$ of the low-energy expansion is retained. Since the coefficients C_i we are interested in, do not depend on the external states one can use the simplest hadronic states for the amplitude calculation, which are the quarks. For the same reason we are allowed to set quark masses to zero and assign to all of them the common value of the space-like momentum $p^2 < 0$. The latter allows us to avoid infrared singularities in the calculation. The diagrams representing the one-loop QCD corrections to the matrix elements of the effective operators in Eq. (16) are shown in Fig 3. In Fig. 2 we give an example of the set

of one-loop diagrams relevant for the calculation of the full theory amplitude. In order to tackle the ultraviolet (UV) divergencies we use the dimensional regularization and the $\overline{\rm MS}$ subtraction scheme. For simplicity we assume that the masses of all the heavy particles of the full theory are equal to a common scale $\Lambda = \Lambda_{LNV}$. Following [14, 15] and for the sake of keeping the discussion simple, in this section we set this matching scale to M_W. Note, however, that given current LHC constraints lower limits on Λ_{LNV} are already of the order of $\Lambda_{LNV} \sim \mathcal{O}(1)$ TeV. We will come back to discuss this in section V. A straightforward calculation shows the general structure of the amplitude and the operator matrix elements in the LO of the QCD perturbation theory has the following form:

$$\mathcal{A}^{Full} = \frac{g_{\rm full}}{\Lambda^5} a_i \left[1 + c_i \frac{\alpha_s}{4\pi}\left(\frac{1}{\epsilon} + \ln\left(\frac{\mu^2}{-p^2}\right)\right) + \frac{\alpha_s}{4\pi} z_i \ln\left(\frac{M_W^2}{-p^2}\right)\right] \langle \mathcal{O}_i \rangle_{\rm tree} \tag{17}$$

$$\langle \mathcal{O}_i \rangle^{(0)} = \left[\delta_{ij} + \frac{\alpha_s}{4\pi} b_{ij}\left(\frac{1}{\epsilon} + \ln\left(\frac{\mu^2}{-p^2}\right)\right)\right] \langle \mathcal{O}_j \rangle_{\rm tree}. \tag{18}$$

Here, $\langle \mathcal{O}_i \rangle_{\rm tree}$ are the operator matrix elements without QCD corrections. The explicit form of the matrix b_{ij} will be given in the LO approximation below. On the other hand, we do not need any knowledge of the coefficients a_i, c_i or z_i since our goal is to calculate the QCD running of the Wilson coefficients of the effective operators, which is determined, as discussed below, by b_{ij} only. The above expression (17) is given in order to clarify some aspects of the matching. The singular $1/\epsilon$ term in Eq. (17) originates from the diagram with the vertex correction Fig. (2a), which is UV divergent, while the diagram Fig. (2b) leads to the finite second term due to the propagators of the virtual heavy particles of the mass $\sim M_W$ cutting the logarithmic divergence at M_W. The singularity from the first term can be eliminated by coupling constant and quark field renormalization. The quark field renormalization due to the QCD corrections is given by

$$q_0 = Z_q^{1/2} q, \quad \text{with} \quad Z_q = 1 - C_F \frac{\alpha_s}{4\pi} \frac{1}{\epsilon} + O(\alpha_s^2), \tag{19}$$

where q_0 and q are the bare and renormalized quark fields with the renormalization constant Z_q given in LO approximation. Here $C_F = (N^2-1)/(2N)$ is the standard $SU(N)$ color factor. In the case of the operator matrix elements in Eq. (18) the $1/\epsilon$-singularities are removed by the quark field renormalization, Eq. (19), accompanied by renormalization of the operators $\mathcal{O}_i^{(0)} = Z_{ij}\mathcal{O}_j$, mixing them within certain groups of the complete list (3)-(7). These groups are identified in the next section. The operator matrix elements in Eq. (18) are renormalized as amputated Green functions

$$\langle \mathcal{O}_i \rangle^{(0)} = Z_q^{-2} Z_{ij} \langle \mathcal{O}_j \rangle. \tag{20}$$

Requiring the cancelation of the singularities in Eq. (18) one finds

$$Z_{ij} = \delta_{ij} + \frac{\alpha_s}{4\pi}(b_{ij} - 2C_F\delta_{ij})\frac{1}{\epsilon} + O(\alpha_s^2). \tag{21}$$

The renormalized matrix elements $\langle \mathcal{O}_j \rangle$ and the amplitude $\mathcal{A}^{Full}$ have the same form as in Eqs. (18), (17), but with $1/\epsilon = 0$ and b_{ij} substituted by $b_{ij} - 2C_F\delta_{ij}$. Inserting these finite quantities in the matching condition, Eq. (16), one finds the Wilson coefficients in the form

$$C_i(\mu) = \left(\delta_{ij} + \frac{\alpha_s}{4\pi} f_{ij} \ln\left(\frac{M_W^2}{\mu^2}\right) + O(\alpha_s^2)\right) C_j^{tree}, \tag{22}$$

where $C_i^{tree} = C_i(M_W)$ are the coefficients derived from a high scale model by integrating out heavy particles and neglecting the QCD corrections. In this formula f_{ij} are some numerical coefficients which explicit form is irrelevant for the present discussion. The above relation is shown in order to motivate the subsequent analysis needed to make contact with $0\nu\beta\beta$ scales, $\mu \sim 100$ MeV. As seen Eq. (22) in this case contains a large logarithmic term breaking the perturbation theory. The way out is very well known: one has to sum up the large logarithms in all orders in α_s on the basis of the Renormalization Group Equations (RGE). It is done in what follows.

B. QCD running of Wilson coefficients

Following Refs. [14, 15] we write the RGE for the Wilson coefficients in matrix form

$$\frac{d\vec{C}(\mu)}{d\ln\mu} = \hat{\gamma}^T \vec{C}(\mu), \tag{23}$$

where $\vec{C} = (C_1, C_2, ...)$ and the anomalous dimension matrix $\hat{\gamma}^T$ is given in the $\overline{\text{MS}}$-scheme by [15] :

$$\hat{\gamma}(\alpha_s) = -2\alpha_s \frac{\partial \hat{Z}_1(\alpha_s)}{\partial \alpha_s}, \tag{24}$$

where $\hat{Z}_1$ is the matrix factor of the singularity $1/\epsilon$ in Eq. (21). Thus we have in the LO approximation

$$\gamma_{ij}(\alpha_s) = \frac{\alpha_s}{4\pi}\gamma_{ij}, \quad \text{with} \quad \gamma_{ij} = -2(b_{ij} - 2C_F\delta_{ij}), \tag{25}$$

where γ_{ij} are the components of the anomalous dimension matrix $\hat{\gamma}$.

The solution of Eq. (23) can be represented in terms of the μ-evolution matrix

$$\vec{C}(\mu) = \hat{U}(\mu, \Lambda) \cdot \vec{C}(\Lambda). \tag{26}$$

between the low and high energy scales μ and Λ, respectively. In the LO one finds

$$\hat{U}(\mu, \Lambda) = \hat{V}\,\text{Diag}\left\{\left[\frac{\alpha_s(\Lambda)}{\alpha_s(\mu)}\right]^{\gamma_i/(2\beta_0)}\right\}\hat{V}^{-1}. \tag{27}$$

The LO QCD running coupling constant is as usual

$$\alpha_s(\mu) = \frac{\alpha_s(\Lambda)}{1 - \beta_0 \frac{\alpha_s(\Lambda)}{2\pi}\log\left(\frac{\Lambda}{\mu}\right)} \tag{28}$$

with $\beta_0 = (33-2f)/3$, where f is the number of the quark flavors with masses $m_f < \mu$. For a normalization we use the experimental value $\alpha_s(\mu = M_z) = 0.118$ [25]. Eq. (27) contains the matrix $\hat{V}$ defined as

$$\text{Diag}\,\{\gamma_i\} = \hat{V}^{-1}\hat{\gamma}\hat{V}, \tag{29}$$

where $\hat{\gamma}$ is the matrix form of γ_{ij}, see Eq. (25). The matrix in the left hand side of Eq. (29) is a diagonal matrix with the diagonal elements γ_i. The same notation is used in Eq. (27).

The quark thresholds in the evolution of the $C_i(\mu)$ down to $\mu_0 \sim 1$ GeV can be approximately taken into account by the chain of the μ-evolution matrices with different numbers, f, of quark flavors:

$$\hat{U}(\mu, \Lambda = M_W) \;=\; \hat{U}^{(f=3)}(\mu_0, \mu_c)\hat{U}^{(f=4)}(\mu_c, \mu_b)\hat{U}^{(f=5)}(\mu_b, M_W), \tag{30}$$

$$\hat{U}(\mu, \Lambda > m_t\;) \;=\; \hat{U}^{(f=3)}(\mu_0, \mu_c)\hat{U}^{(f=4)}(\mu_c, \mu_b)\hat{U}^{(f=5)}(\mu_b, \mu_t)\hat{U}^{(f=6)}(\mu_t, \Lambda), \tag{31}$$

for two cases of the high energy scale Λ considered in the present paper. Here $\hat{U}^{(f)}$ are the matrix $\hat{U}$ in Eq. (27) calculated for $f = 3, 4, 5, 6$ quark flavors. The intermediate scales we simply put to the corresponding quark thresholds $\mu_c = m_c, \mu_b = m_b, \mu_t = m_t$, which is an adequate appropriation for the LO analysis (for more details see refs. [14, 15]).

C. Leading order QCD running of the $0\nu\beta\beta$ operator basis

In the leading order, the QCD corrections of the effective operators of the $0\nu\beta\beta$ basis are shown in Fig.3. Of course, other similar 1-loop diagrams with all other possible gluon links of the quark legs have to be taken into account additionally. The diagrams (a), (b), (c), counted from the left to the right, contribute to the operator matrix elements (18) with the following structures

$$\text{(a)} \;\sim\; (\bar{u}\Gamma^i P_X d)\;\cdot\;(\bar{u}\gamma_\alpha\gamma_\beta\Gamma^j\gamma^\beta\gamma^\alpha P_Y d)\;\cdot\; j_{\mathcal{O}}\;\cdot\; C_F\frac{1}{4}\frac{\alpha}{4\pi}\left(\frac{1}{\epsilon} + \log\frac{\mu^2}{-p^2}\right) \tag{32}$$

$$\text{(b)} \;\sim\; -(\bar{u}\Gamma^i\gamma_\sigma\gamma_\alpha T^a P_X d)\;\cdot\;(\bar{u}\Gamma^j\gamma^\sigma\gamma^\alpha T^a P_Y d)\;\cdot\; j_{\mathcal{O}}\;\cdot\; \frac{1}{4}\frac{\alpha}{4\pi}\left(\frac{1}{\epsilon} + \log\frac{\mu^2}{-p^2}\right) \tag{33}$$

$$\text{(c)} \;\sim\; (\bar{u}\Gamma^i\gamma_\sigma\gamma_\alpha T^a P_X d)\;\cdot\;(\bar{s}\gamma^\alpha\gamma^\sigma\Gamma^j T^a P_Y d)\;\cdot\; j_{\mathcal{O}}\;\cdot\; \frac{1}{4}\frac{\alpha}{4\pi}\left(\frac{1}{\epsilon} + \log\frac{\mu^2}{-p^2}\right), \tag{34}$$

where Γ^i are the Lorentz structures corresponding to the operators from Eqs. (3)-(7) with the leptonic currents $j_{\mathcal{O}}$, see Eq. (8) and T^a are the generators of $SU(3)$. Using Eq. (25) we find the LO anomalous dimensions for all the $0\nu\beta\beta$-operators as

$$\hat{\gamma}^{XY}_{(31)} = -2\begin{pmatrix} -\frac{3}{N} & -6 \\ 0 & 6C_F \end{pmatrix}, \qquad \hat{\gamma}^{XX}_{(12)} = -2\begin{pmatrix} 6C_F - 3 & \frac{1}{2N} + \frac{1}{4} \\ -12 - \frac{24}{N} & -3 - 2C_F \end{pmatrix} \tag{35}$$

$$\gamma^{XX}_{(3)} = -2\left(\frac{3}{N} - 3\right), \qquad \gamma^{XY}_{(5)} = -3\gamma^{XY}_{(4)} = -12\,C_F, \tag{36}$$

$$\hat{\gamma}^{XX}_{(45)} = -2\begin{pmatrix} 9 - 2C_F & 3i - \frac{6i}{N} \\ i + \frac{2i}{N} & 6C_F + 1 \end{pmatrix}, \tag{37}$$

where the superscripts $X \neq Y = L, R$ denote the chiralities while the subscripts the numbers of the operators from Eqs. (3)-(7) mixed under the renormalization. For instance, the first matrix mixes the operators $\mathcal{O}_3^{XY}, \mathcal{O}_1^{XY}$ with $X \neq Y = L, R$, and so on. The anomalous dimensions in the second row (36) are just numbers renormalizing each of the operators $\mathcal{O}_3^{XX}$, $\mathcal{O}_{5,4}^{XY}$ separately without mixing. Then, using Eqs. (27)-(30) one can find the μ-evolution matrix $U(\mu, M_W)$ and explicitly relate the Wilson coefficients at high- and low-energy scales.

V. QCD CORRECTED $0\nu\beta\beta$ HALF-LIFE AND LIMITS ON HIGH-SCALE MODELS

Now we express the half-life of $0\nu\beta\beta$-decay Eq. (9) in terms of the high-scale $C_i(\Lambda)$ Wilson coefficients. This is the central result of the present paper:

$$\begin{aligned}\left[T_{1/2}^{0\nu\beta\beta}\right]^{-1} \;=\; & G_1 \Big|\beta_1^{XX}\left(C_1^{LL}(\Lambda)+C_1^{RR}(\Lambda)\right)+\beta_1^{LR}\left(C_1^{LR}(\Lambda)+C_1^{RL}(\Lambda)\right)+ \\ & +\beta_2^{XX}\left(C_2^{LL}(\Lambda)+C_2^{RR}(\Lambda)\right)+ \\ & +\beta_3^{XX}\left(C_3^{LL}(\Lambda)+C_3^{RR}(\Lambda)\right)+\beta_3^{LR}\left(C_3^{LR}(\Lambda)+C_3^{RL}(\Lambda)\right)\Big|^2+ \\ +\; & G_2 \Big|\beta_4^{XX}\left(C_4^{RR}(\Lambda)+C_4^{RR}(\Lambda)\right)+\beta_4^{LR}\left(C_4^{LR}(\Lambda)+C_4^{RL}(\Lambda)\right)+ \\ & +\beta_5^{XX}\left(C_5^{RR}(\Lambda)+C_5^{RR}(\Lambda)\right)+\beta_5^{LR}\left(C_5^{LR}(\Lambda)+C_5^{RL}(\Lambda)\right)\Big|^2 ,\end{aligned} \tag{38}$$

where

$$\beta_1^{XX} = \mathcal{M}_1\;\; U_{(12)11}^{XX}+\mathcal{M}_2 U_{(12)21}^{XX}, \quad \beta_1^{LR}=\mathcal{M}_3^{(+)}U_{(31)12}^{LR}+\mathcal{M}_1 U_{(31)22}^{LR}, \tag{39}$$

$$\beta_2^{XX} = \mathcal{M}_1\;\; U_{(12)12}^{XX}+\mathcal{M}_2 U_{(12)22}^{XX}, \tag{40}$$

$$\beta_3^{XX} = \mathcal{M}_3^{(-)}U_{(3)}^{XX}, \qquad \beta_3^{LR}=\mathcal{M}_3^{(+)}U_{(31)11}^{LR} \tag{41}$$

$$\beta_4^{XX} = -|\mathcal{M}_4|\;\; U_{(45)11}^{XX}+|\mathcal{M}_5|\,U_{(45)21}^{XX}, \quad \beta_4^{LR}=|\mathcal{M}_4|\,U_{(4)}^{LR}, \tag{42}$$

$$\beta_5^{XX} = -|\mathcal{M}_4|\;\; U_{(45)12}^{XX}+|\mathcal{M}_5|\,U_{(45)22}^{XX}, \quad \beta_5^{LR}=|\mathcal{M}_5|\,U_{(5)}^{LR}. \tag{43}$$

From Eqs. (3) and (5) one sees that $\mathcal{O}_1^{XY}$ and $\mathcal{O}_3^{XY}$ are symmetric under the interchange of X and Y. Consequently, in Eq. (38) $C_1^{LR}=C_1^{RL}$ and $C_3^{LR}=C_3^{RL}$, which is equivalent to a factor 2. Coherently with Eqs. (35)-(37) the subscripts of the evolution matrix U in the parenthesis denote the subscripts of the operators from Eqs. (3)-(7) mixed under the renormalization, the subscripts without the parenthesis specify the matrix element. Numerical values of these matrix elements are given in Appendix A. The nuclear matrix elements $\mathcal{M}_i$ are defined in Ref. [4] and can be calculated in any nuclear structure model. We use their numerical values as given in Ref. [2] and display them for convenience in Table I.

The currently best lower bounds on the $0\nu\beta\beta$-decay half-life come from experiments using ^{76}Ge (combined GERDA and Heidelberg–Moscow limits) [10] and ^{136}Xe (combined EXO and

^{A}X	$\mathcal{M}_1$	$\mathcal{M}_2$	$\mathcal{M}_3^{(+)}$	$\mathcal{M}_3^{(-)}$	$\lvert\mathcal{M}_4\rvert$	$\lvert\mathcal{M}_5\rvert$
^{76}Ge	9.0	-1.6×10^3	1.3×10^2	2.1×10^2	$\lvert 1.9 \times 10^2\rvert$	$\lvert 1.9 \times 10^1\rvert$
^{136}Xe	4.5	-8.5×10^2	6.9×10^1	1.1×10^2	$\lvert 9.6 \times 10^1\rvert$	$\lvert 9.3\rvert$

TABLE I: The numerical values of the nuclear matrix elements $\mathcal{M}_i$ taken from Ref. [2].

KamlandZEN limits) [13]. We use:

$$T_{1/2}^{0\nu\beta\beta}(^{76}Ge) \geq T_{1/2}^{0\nu\beta\beta-exp}(^{76}Ge) = 3.0\ 10^{25}\ \text{yrs}, \tag{44}$$

$$T_{1/2}^{0\nu\beta\beta}(^{136}Xe) \geq T_{1/2}^{0\nu\beta\beta-exp}(^{136}Xe) = 3.4\ 10^{25}\ \text{yrs}. \tag{45}$$

From these experimental lower bounds we derive upper limits on $C_i(\Lambda)$ using Eq. (38). Since the $d = 9$ effective operators contributing to the short-range mechanism of $0\nu\beta\beta$ are generated at the mass scale of the heavy particles and considering that the LHC gives limits of the order of $\Lambda_{LNV} \sim 1$ TeV, we also present the limits on $C_i(\Lambda_{LNV})$. The results are shown in Table II, where we also present, for comparison, the "old limits" $C_i^{(0)}$ neglecting the QCD running, but updated with the new half-live limits as given in Eqs (44) and (45). Neglecting the QCD running corresponds to setting $U_{ij}^{XY} = \delta_{ij}$ in Eqs. (39)-(43).

We assumed for simplicity that there are no significant cancellations between the terms in the right-hand sides of Eq. (38). Comparing the different numbers, one sees that the running between M_W and $\mu_0 \simeq 1$ GeV is more important than the running between 1 TeV and M_W, but the latter is not negligible. As can also be seen from Table II, the QCD RGE running has the largest impact on the contributions to the operators $\mathcal{O}_1^{XX}$ and $\mathcal{O}_5^{XX}$. This can be understood since their RGE mix with the operators $\mathcal{O}_2^{XX}$ and $\mathcal{O}_4^{XX}$, respectively, which have significantly larger nuclear matrix elements, as seen from Table I.

If one is interested in constraining a particular high-scale model such as, for example, the scalar exchange considered in sec. III, the corresponding limits on the model parameters in certain cases can be more stringent than in Table II. For example, the model specified in Eq. (12) with $S_{8,2,1/2}$ contains two non-vanishing Wilson coefficients at the matching scale, $C_1^{RR}(\Lambda)$ and $C_2^{RR}(\Lambda)$, which obey the relation $C_2^{RR} = (3/20)C_1^{RR}$. Since the individual limit on C_2^{RR} is weaker than the one on C_1^{RR}, the upper limit on the total C_1^{RR} in this model is only about 2% better than in Table II. For all models listed in [9] one can find QCD improved limits in the same manner. Note, however, that for other models the changes of the limits, after taking into account both operators, can be much larger than in our example model.

VI. CONCLUSIONS

In this paper we have calculated QCD corrections to the complete list of Lorentz-invariant operators for the short-range (SR) part of the $0\nu\beta\beta$ decay amplitude. We have used the RGE technique to derive 1-loop improved limits on all the Wilson coefficients appearing in the SR contributions to $0\nu\beta\beta$ decay. We stress again, that we have taken special care to

^{A}X	$\lvert C_1^{XX}(\Lambda_1)\rvert$	$\lvert C_1^{XX}(\Lambda_2)\rvert$	$\lvert C_1^{XX(0)}\rvert$	$\lvert C_1^{LR,RL}(\Lambda_1)\rvert$	$\lvert C_1^{LR,RL}(\Lambda_2)\rvert$	$\lvert C_1^{LR,RL(0)}\rvert$
^{76}Ge	5.0×10^{-10}	3.8×10^{-10}	2.6×10^{-7}	1.5×10^{-8}	9.1×10^{-9}	2.6×10^{-7}
^{136}Xe	3.4×10^{-10}	2.6×10^{-10}	1.8×10^{-7}	9.7×10^{-9}	6.1×10^{-9}	1.8×10^{-7}
^{A}X	$\lvert C_2^{XX}(\Lambda_1)\rvert$	$\lvert C_2^{XX}(\Lambda_2)\rvert$	$\lvert C_2^{XX(0)}\rvert$	–		
^{76}Ge	3.5×10^{-9}	5.2×10^{-9}	1.4×10^{-9}	–		
^{136}Xe	2.4×10^{-9}	3.5×10^{-9}	9.4×10^{-10}	–		
^{A}X	$\lvert C_3^{XX}(\Lambda_1)\rvert$	$\lvert C_3^{XX}(\Lambda_2)\rvert$	$\lvert C_3^{XX(0)}\rvert$	$\lvert C_3^{LR,RL}(\Lambda_1)\rvert$	$\lvert C_3^{LR,RL}(\Lambda_2)\rvert$	$\lvert C_3^{LR,RL(0)}\rvert$
^{76}Ge	1.5×10^{-8}	1.6×10^{-8}	1.1×10^{-8}	2.0×10^{-8}	2.1×10^{-8}	1.8×10^{-8}
^{136}Xe	9.7×10^{-9}	1.1×10^{-8}	7.4×10^{-9}	1.4×10^{-8}	1.4×10^{-8}	1.2×10^{-8}
^{A}X	$\lvert C_4^{XX}(\Lambda_1)\rvert$	$\lvert C_4^{XX}(\Lambda_2)\rvert$	$\lvert C_4^{XX(0)}\rvert$	$\lvert C_4^{LR,RL}(\Lambda_1)\rvert$	$\lvert C_4^{LR,RL}(\Lambda_2)\rvert$	$\lvert C_4^{LR,RL(0)}\rvert$
^{76}Ge	5.0×10^{-9}	3.9×10^{-9}	1.2×10^{-8}	1.7×10^{-8}	1.9×10^{-8}	1.2×10^{-8}
^{136}Xe	3.4×10^{-9}	2.7×10^{-9}	7.9×10^{-9}	1.2×10^{-8}	1.3×10^{-8}	7.9×10^{-9}
^{A}X	$\lvert C_5^{XX}(\Lambda_1)\rvert$	$\lvert C_5^{XX}(\Lambda_2)\rvert$	$\lvert C_5^{XX(0)}\rvert$	$\lvert C_5^{LR,RL}(\Lambda_1)\rvert$	$\lvert C_5^{LR,RL}(\Lambda_2)\rvert$	$\lvert C_5^{LR,RL(0)}\rvert$
^{76}Ge	2.3×10^{-8}	1.4×10^{-8}	1.2×10^{-7}	3.9×10^{-8}	2.8×10^{-8}	1.2×10^{-7}
^{136}Xe	1.6×10^{-8}	9.5×10^{-9}	8.2×10^{-8}	2.8×10^{-8}	2.0×10^{-8}	8.2×10^{-8}

TABLE II: Upper limits on the Wilson coefficients in Eq. (38) with $C_i(\Lambda)$ calculated for two different matching scales, $\Lambda_1 = M_W$ and $\Lambda_2 = \Lambda_{LNV} = 1$ TeV. For comparison we also give $C_i^{(0)}$, i.e. limits without QCD running.

present our results in such a way, that improved limits can be derived easily, should updated experimental limits or improved nuclear physics calculations become available.

Our numerical results show that the QCD corrections are indeed important. We note that both more and less stringent limits can result from taking into account QCD corrections, depending on the operator under consideration. In particular, the appearance of color mismatched operators lead to operator mixing which, due to largely different nuclear matrix elements for different operators, can lead to surprisingly large changes in some limits. QCD improved limits from $0\nu\beta\beta$ decay should therefore be used, when comparing constraints from $0\nu\beta\beta$ decay with those derived from LHC.

Acknowledgements

M.G. thanks the IFIC for hospitality during her stay. This work was supported by the Spanish MICINN grants FPA2014-58183-P and Multidark CSD2009-00064 (MINECO), and PROMETEOII/2014/084 (Generalitat Valenciana), and by Fondecyt (Chile) under grants 1150792 and 3160642.

I. APPENDIX A. EXPLICIT FORM OF THE EVOLUTION MATRIX.

Here we give the numeric values of the μ-evolution matrix elements defined in Eq. (27) and taking into account the quark thresholds according to (30). In the notations used in

Eqs. (39)-(43) we have for two reference values , $\Lambda_1 = M_W$ and $\Lambda_2 = 1$ TeV, of the high energy scale Λ, and $\mu_0 = 1$ Gev, the following results

$$\hat{U}^{XX}_{(12)}(\mu_0, \Lambda_1) = \begin{pmatrix} 1.88 & 0.06 \\ -2.76 & 0.40 \end{pmatrix}, \quad U^{XX}_{(3)}(\mu_0, \Lambda_1) = 0.76, \tag{A.1}$$

$$\hat{U}^{LR}_{(31)}(\mu_0, \Lambda_1) = \begin{pmatrix} 0.87 & -1.40 \\ 0 & 2.97 \end{pmatrix}, \quad \hat{U}^{XX}_{(45)}(\mu_0, \Lambda_1) = \begin{pmatrix} 2.33 & 0.39i \\ 0.64i & 3.35 \end{pmatrix}, \tag{A.2}$$

$$U^{LR}_{(4)}(\mu_0, \Lambda_1) = 0.70, \qquad U^{LR}_{(5)}(\mu_0, \Lambda_1) = 2.97\,. \tag{A.3}$$

and

$$\hat{U}^{XX}_{(12)}(\mu_0, \Lambda_2) = \begin{pmatrix} 2.24 & 0.07 \\ -3.70 & 0.27 \end{pmatrix}, \quad U^{XX}_{(3)}(\mu_0, \Lambda_2) = 0.70, \tag{A.4}$$

$$\hat{U}^{LR}_{(31)}(\mu_0, \Lambda_2) = \begin{pmatrix} 0.84 & -2.19 \\ 0 & 4.13 \end{pmatrix}, \quad \hat{U}^{XX}_{(45)}(\mu_0, \Lambda_2) = \begin{pmatrix} 2.98 & 0.69i \\ 1.15i & 4.82 \end{pmatrix}, \tag{A.5}$$

$$U^{LR}_{(4)}(\mu_0, \Lambda_2) = 0.62, \qquad U^{LR}_{(5)}(\mu_0, \Lambda_2) = 4.13\,. \tag{A.6}$$

---

[1] I. Avignone, Frank T., S. R. Elliott, and J. Engel, Rev.Mod.Phys. **80**, 481 (2008), arXiv:0708.1033.

[2] F. F. Deppisch, M. Hirsch, and H. Päs, J.Phys. **G39**, 124007 (2012), arXiv:1208.0727.

[3] H. Päs, M. Hirsch, H. Klapdor-Kleingrothaus, and S. Kovalenko, Phys.Lett. **B453**, 194 (1999).

[4] H. Päs, M. Hirsch, H. Klapdor-Kleingrothaus, and S. Kovalenko, Phys.Lett. **B498**, 35 (2001), arXiv:hep-ph/0008182.

[5] K. Babu and R. Mohapatra, Phys.Rev.Lett. **75**, 2276 (1995), arXiv:hep-ph/9506354.

[6] M. Hirsch, H. Klapdor-Kleingrothaus, and S. Kovalenko, Phys.Lett. **B372**, 181 (1996), arXiv:hep-ph/9512237.

[7] H. Päs, M. Hirsch, and H. Klapdor-Kleingrothaus, Phys.Lett. **B459**, 450 (1999), arXiv:hep-ph/9810382.

[8] M. Hirsch, H. Klapdor-Kleingrothaus, and S. Kovalenko, Phys.Rev. **D54**, 4207 (1996), arXiv:hep-ph/9603213.

[9] F. Bonnet, M. Hirsch, T. Ota, and W. Winter, JHEP **1303**, 055 (2013), arXiv:1212.3045.

[10] GERDA Collaboration, M. Agostini et al., Phys.Rev.Lett. **111**, 122503 (2013), arXiv:1307.4720.

[11] EXO-200 Collaboration, J. Albert et al., Nature **510**, 229234 (2014), arXiv:1402.6956.

[12] KamLAND-Zen Collaboration, I. Shimizu, Neutrino 2014, Boston (2014).

[13] KamLAND-Zen Collaboration, A. Gando et al., Phys. Rev. Lett. **110**, 062502 (2013), arXiv:1211.3863.

[14] G. Buchalla, A. J. Buras, and M. E. Lautenbacher, Rev.Mod.Phys. **68**, 1125 (1996), arXiv:hep-ph/9512380.

[15] A. J. Buras, Weak Hamiltonian, CP violation and rare decays, Probing the standard model of particle interactions. Proceedings, Summer School in Theoretical Physics, NATO Advanced Study Institute, 68th session, Les Houches, France, July 28-September 5, 1997. Pt. 1, 2, pp. 281–539, 1998, arXiv:hep-ph/9806471.

[16] N. Mahajan, Phys.Rev.Lett. **112**, 031804 (2014).

[17] T. Peng, M. J. Ramsey-Musolf, and P. Winslow, (2015), arXiv:1508.04444.

[18] M. Doi, T. Kotani, and E. Takasugi, Prog.Theor.Phys.Suppl. **83**, 1 (1985).

[19] K. Muto, E. Bender, and H. Klapdor, Z.Phys. **A334**, 187 (1989).

[20] A. Faessler, M. González, S. Kovalenko, and F. Simkovič, Phys.Rev. **D90**, 096010 (2014), arXiv:1408.6077.

[21] J. Hyvrinen and J. Suhonen, Phys.Rev. **C91**, 024613 (2015).

[22] J. Menendez, A. Poves, E. Caurier, and F. Nowacki, J.Phys.Conf.Ser. **312**, 072005 (2011).

[23] M. Blennow, E. Fernandez-Martinez, J. Lopez-Pavon, and J. Menendez, JHEP **1007**, 096 (2010), arXiv:1005.3240.

[24] R. Sen'kov and M. Horoi, Phys.Rev. **C90**, 051301 (2014), arXiv:1411.1667.

[25] Particle Data Group, J. Beringer et al., Phys.Rev. **D86**, 010001 (2012).